Asociación Argentina
de Mecánica Computacional

Mecánica Computacional Vol XXIX, págs. 4377-4387 (artículo completo)
Eduardo Dvorkin, Marcela Goldschmit, Mario Storti (Eds.)
Buenos Aires, Argentina, 15-18 Noviembre 2010

DYNAMIC POSITIONAL FINITE ELEMENT METHOD APPLIED TO NONLINEAR GEOMETRIC 3D SOLIDS

Daniel N. Maciel[a], **Humberto B. Coda**[b]

[a]*Escola de Ciências e Tecnologia, Universidade Federal do Rio Grande do Norte, Campus Universitário Lagoa Nova - Natal - RN, Brazil, dnmaciel@ect.ufrn.br, http://www.ect.ufrn.br/node/326*

[b]*Escola de Engenharia de São Carlos, Universidade de São Paulo, São Carlos-SP, Brazil, hbcoda@sc.usp.br, http://www.set.eesc.usp.br/public/pessoas/professor.php?id=8*

Keywords: Solids, Geometric nonlinearity, dynamic problems, finite elements.

Abstract. This paper presents the dynamic positional nonlinear geometric formulation for tridimensional problems. The positional formulation is an alternative approach for non linear problems, since it considers nodal positions as variables of the nonlinear system instead of displacements as usual in literature. In order to avoid locking, tetrahedral third-order isoparametric finite element (20 nodes) is implemented for both displacement and stress field. Regarding to dynamic forces, it is considered the consistent mass matrix and damping effects proportional to the body mass. The well-known Newmark algorithm for time integration is applied. Some simple numerical examples are presented in order to show the accuracy of the proposed formulation.

1 INTRODUCTION

Most structural elements that may suffer large displacements generally have one of the three dimensions much smaller than the others. Therefore, it is very common to find in the literature of nonlinear geometric problems involving three-dimensional solid in its purest form, i.e., without any kinematic assumption to represent structures like shells, plates, or even space frame.

Moreover, with the growing progress of the study of biomechanics, it is necessary to consider problems with three-dimensional solids, because the structural components, represented by muscles and internal organs of human body such as the heart, arteries and even the ocular globe, may suffer sometimes large deformations and displacements. For example, the work of Haussy and Ganghoffer (2005) analyses the instability of thick wall shells, that can simulates an artery aneurysm with use of an appropriate constitutive law concerning the nature of the deformed structure (large displacements and large deformations). In Hron and Mádlik (2006), a fluid-structure coupling formulation applied to problems in biomechanics is shown with solid tetrahedral elements of 10 nodes (quadratic approximation of variables).

In addition, formulations employing cylindrical coordinates and polar rather than Cartesian coordinates are employed to solve problems involving tires. It is presented in Danielson and Ahmed (1997) that developed a formulation for the tire contact with pavement using a 4-node hexahedrical cylindrical element. The same type of formulation in cylindrical coordinates can also be found in Bourdais et al. (2003) and Costa et al (1996).

With regard to the variables approximation in solids to represent large displacements and deformations, there are many works that developed formulations using linear element approximation, and to overcome the locking effect caused by low-order polynomial approach, strategies for improving the stress and strain field are commonly employed. That is the case of works such as Simo et al (1993), Simo and Armero (1992), Armero and Garikipati (1996), Moita and Crisfield (1996) and Reese et al (1999) that used a strategy to improve the strain field called *enhanced strains field.* In Kozar and Ibrahimbegović (1995) and in Simo and Armero (1992) , in order to alleviate locking, the incompatible modes technique is applied, and it means to assume that the gradient of displacements is optimized by adding another incompatible gradient, i.e., which is discontinuous over the element, but consistent in the variational aspect.

Despite the papers described above have focused on low-order elements, in Rank et al (1998) and Düster et al (2003) conclude that eliminate locking problems, it is enough to employ high order elements. The authors share that philosophy, so the solid element used here is the 20-node tetrahedral, creating a cubic approximation of variables and fields without the use optimized strain or tension field.

The static positional formulation for solids has already been presented in Maciel and Coda (2009). Thus, herein is showed the positional formulation regarding dynamic problems. Classical examples found in literature are presented.

2 POSITIONAL DYNAMIC FORMULATION

2.1 Energetic Approach

The positional formulation starts with the energetic approach, that is, the total potencial energy concept is applied for total lagrangian description and given by:

$$\Pi = U_e + K_c + K_a - P \tag{1}$$

Where U_e and P are the elastic potential energy and potential energy of the external forces respectively. K_c is the kinetic energy of the body and K_a is the energy loss due to damping effects. The elastic potential energy U_e is:

$$U_e = \int_{V_0} u_e dV_0 \tag{2}$$

where u_e is specific elastic energy and V_0 is the total volume of the body in the reference configutarion (total lagrangian). Moreover, for the kinetic energy, one can write:

$$K_c = \int_{V_0} \rho_0 \frac{\dot{x}_i \dot{x}_i}{2} dV_0 \tag{3}$$

where ρ_0 is the specific mass of the body and $\dot{\mathbf{x}}$ is the vetorial velocity of a generic point, given by:

$$\dot{\mathbf{x}} = \frac{d(\mathbf{x})}{dt} \tag{4}$$

and **x** is the position vector of the generic point.

The potential energy of the external forces can be written as:

$$P = \mathbf{F}^T \mathbf{X} \tag{5}$$

where **F** is the vector of the external forces and **X** the respective position vector.

Regarding to the energy loss due to damping effects, one can write:

$$\frac{\partial K_a}{\partial x_i} = \int_{V_0} \frac{\partial k_a}{\partial x_i} dV_0 = \int_{V_0} c_m \rho_0 \dot{x}_i dV_0 \tag{6}$$

where c_m is the damping coefficient.

By replacing Eq. (2), Eq.(3), Eq.(5) and Eq.(6) in Eq.(1), the total potential energy becomes:

$$\Pi = \int_{V_0} u_e dV_0 + \int_{V_0} \rho_0 \frac{\dot{x}_i \dot{x}_i}{2} dV_0 - F_j X_j + K_a \tag{7}$$

In order achieve equilibrium in current time step "S+1" (time "S" is the former time step), the energy functional must be a minimum, that is:

$$\left.\frac{\partial \Pi}{\partial x_i}\right|_{S+1} = \int_{V_0} \frac{\partial u_e}{\partial x_i} dV_0 + \int_{V_0} \frac{\partial}{\partial x_i}\left(\rho_0 \frac{\dot{x}_k \dot{x}_k}{2}\right) dV_0 - \frac{\partial F_j X_j}{\partial x_i} + \frac{\partial K_a}{\partial x_i} = 0 \tag{8}$$

Taking into account Eq. (6), Eq.(8) becomes:

$$\left.\frac{\partial \Pi}{\partial x_i}\right|_{s+1} = \int_{V_0} \frac{\partial u_e}{\partial x_i} dV_0 + \int_{V_0} \frac{\partial}{\partial x_i}\left(\rho_0 \frac{\dot{x}_k \dot{x}_k}{2}\right) dV_0 - F_i + \int_{V_0} c_m \rho_0 \dot{x}_i dV_0 = 0 \tag{9}$$

When the body or structure is discretized in finite elements, its variables, in this case positions, velocities, accelerations and stress field along a generic finite element, can be expressed by assuming shape functions, as shown:

$$x_i = \Phi_j X_i^j \tag{10}$$

$$\dot{x}_i = \Phi_j \dot{X}_i^j \tag{11}$$

$$\ddot{x}_i = \Phi_j \ddot{X}_i^j \tag{12}$$

where X_i, $\dot{X}_i$ e $\ddot{X}_i$ are respectively nodal values for positions, velocities and accelerations, and Φ_j the shape functions. By considering, however, approximated variables through shape functions given by Eq.(10), Eq.(11) and Eq.(12), one may write the Eq.(9) as follows:

$$\left.\frac{\partial \Pi}{\partial X}\right|_{S+1} = \left.\frac{\partial U_e}{\partial X}\right|_{S+1} - F_{S+1} + \mathbf{M}\ddot{\mathbf{X}}_{S+1} + \mathbf{C}\dot{\mathbf{X}}_{S+1} = 0 \tag{13}$$

where the Mass Matrix is given by:

$$\mathbf{M} = \int_{V_0} \rho_0 \Phi_k \Phi_j dV_0 \tag{14}$$

and damping matrix (proportional to the body mass):

$$\mathbf{C} = 2c_m \mathbf{M} \tag{15}$$

where c_m is the damping coefficient.

2.2 Iterative solution for the dynamic problem

The Eq.(13) is the nonlinear movement equation, and in order to solve it along the time, the current variables positions and velocities in time step "S+1" are approximated according to the Newmark expressions, that is:

$$X_{S+1} = X_S + \Delta t \dot{X}_S + \Delta t^2 \left[\left(\frac{1}{2} - \beta \right) \ddot{X}_S + \beta \ddot{X}_{S+1} \right] \tag{16}$$

$$\dot{X}_{S+1} = \dot{X}_S + \Delta t (1-\gamma) \ddot{X}_S + \gamma \Delta t \ddot{X}_{S+1} \tag{17}$$

where γ and β the Newmark coefficients that determine how the variables velocities and positions vary along the time interval Δt. One may isolate the current acceleration term in Eq.(16), thus:

$$\ddot{X}_{S+1} = \frac{X_{S+1}}{\beta \Delta t^2} - \frac{X_S}{\beta \Delta t^2} - \frac{\dot{X}_S}{\beta \Delta t} - \left(\frac{1}{2\beta} - 1 \right) \ddot{X}_S \tag{18}$$

Therefore, by replacing Eq.(17) and Eq.(18) in Eq.(13), one has:

$$\left.\frac{\partial \Pi}{\partial X}\right|_{S+1} = \left.\frac{\partial U_t}{\partial X}\right|_{S+1} - F_{S+1} + \frac{M}{\beta \Delta t^2} X_{S+1} - MQ_S + CR_S + \frac{\gamma C}{\beta \Delta t} X_{S+1} - \gamma \Delta t C Q_S = 0 \tag{19}$$

where the vectors Q_S and R_S are related to the variables past contributions (step "S") and given by:

$$Q_S = \frac{X_S}{\beta \Delta t^2} + \frac{\dot{X}_S}{\beta \Delta t} + \left(\frac{1}{2\beta} - 1 \right) \ddot{X}_S \tag{20}$$

$$R_S = \dot{X}_S + \Delta t (1-\gamma) \ddot{X}_S \tag{21}$$

By deriving Eq.(19) related to the nodal positions, one has the Hessian Matrix for the dynamic problem:

$$\left.\frac{\partial^2 \Pi}{\partial X^2}\right|_{S+1} = \nabla g(X_0) = \left.\frac{\partial^2 U_t}{\partial X^2}\right|_{S+1} + \frac{M}{\beta \Delta t^2} + \frac{\gamma C}{\beta \Delta t} \tag{22}$$

Since Eq.(22) represents the nonlinear system to be solved in current time "S+1", the Newton-Raphason Method is applied. By performing the Taylor expansion one has:

$$\mathbf{g(X) = 0 \cong g(X_0) + \nabla g(X_0)\Delta X} \tag{23}$$

or

$$\mathbf{\Delta X = -[\nabla g(X_0)]^{-1} g(X_0)} \tag{24}$$

where the vector $\mathbf{X}$ is the unknown positions vector and $\mathbf{X}_0$ the tentative vector. The unbalanced force of the mechanical system is obtained form Eq.(19) and given by:

$$g(X_0) = \left.\frac{\partial U_t}{\partial X}\right|_{S+1} - F_{S+1} + \frac{M}{\beta \Delta t^2} X_{S+1} - MQ_S + CR_S + \frac{\gamma C}{\beta \Delta t} X_{S+1} - \gamma \Delta t C Q_S \tag{25}$$

In addition, during the iterative process, positions must be updated as shown:

$$X_{S+1} = X_S + \Delta X \tag{26}$$

Followed by respective accelerations:

$$\ddot{X}_{S+1} = \frac{X_{S+1}}{\beta \Delta t^2} - Q_S \tag{27}$$

3 POSITIONAL FEM DYNAMIC FORMULATION FOR SOLIDS

3.1 Geometry Mapping and Strain Measure

In order to mapping the body movement along space and time, it is considered, according to Figure 1, the position $\mathbf{B}_0$ of the body, which is referred to the reference position and **B** that is related to the current position.

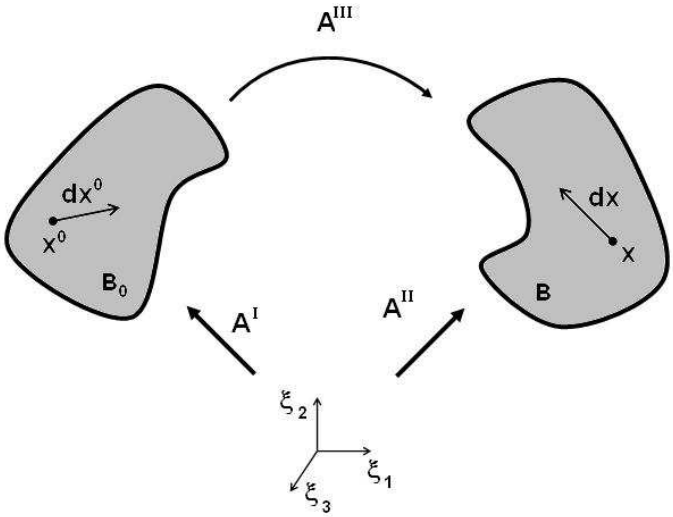

Figure 1: Geometry mapping scheme for the tridimensional solid

$\mathbf{A^{III}}$ are deformation gradient of two positions, i.e., the reference and current positions. Moreover, $\mathbf{A^{I}}$, $\mathbf{A^{II}}$ are auxiliary deformation gradients that represent the deformation between the non dimensional space in respect to the reference configuration and current configuration respectively.

The deformation gradient from $\mathbf{B}_0$ to **B** can be written as:

$$A_{ik}^{III} = \frac{dx_i}{dx_k^0} \tag{28}$$

where $\mathbf{dx}^0$ and $\mathbf{dx}$ are two infinitesimal vectors in the initial and current configuration.

And both auxiliaries deformation gradients are:

$$A_{ik}^{I} = \frac{dx_i^0}{d\xi_k} \tag{29}$$

$$A_{ik}^{II} = \frac{dx_i}{d\xi_k} \tag{30}$$

From those auxiliaries deformation gradients, one can write the deformation gradient $\mathbf{A}^{\mathbf{III}}$, as follows:

$$A_{ik}^{III} = \frac{dx_i}{d\xi_j}\frac{d\xi_j}{dx_k^0} = \frac{dx_i}{dx_k^0} = A_{ik}^{II}\left(A_{ik}^{I}\right)^{-1} \tag{31}$$

The stretch can be written as (Ogden, 1984):

$$\lambda(\mathbf{M}) = \frac{|\mathbf{dx}|}{|\mathbf{dx^0}|} = \left[\mathbf{M}\left(\mathbf{A}^{\mathbf{T}}\mathbf{A}\mathbf{M}\right)\right]^{1/2} \tag{32}$$

where $\mathbf{M}$ is the versor along fiber $\mathbf{dx}^0$. Taking into account Eq.(32), for the global reference x_1, x_2 and x_3,one can write:

$$\lambda_k = \left[\mathbf{e}_{(k)}^{\mathbf{T}}\left(\mathbf{A}^{\mathbf{III}}\right)^{\mathrm{T}}\mathbf{A}^{\mathbf{III}}\mathbf{e}_{(k)}\right]^{1/2} \tag{33}$$

where $\mathbf{e}_1$, $\mathbf{e}_2$ and $\mathbf{e}_3$ are the respective global coordinates versors. Therefore, the engineering deformation (Maciel and Coda, 2009) is written as:

$$\varepsilon_k = \lambda_k - 1 = \left[\mathbf{e}_{(k)}^{\mathbf{T}}\left(\mathbf{A}^{\mathbf{III}}\right)^{\mathrm{T}}\mathbf{A}^{\mathbf{III}}\mathbf{e}_{(k)}\right]^{1/2} - 1 \tag{34}$$

and the distortion:

$$\gamma_{ij} = \theta_{ij} - \frac{\pi}{2} = a\cos\left[\frac{\mathbf{e}_i \bullet \left(\left(\mathbf{A}^{\mathrm{III}}\right)^{\mathbf{T}}\mathbf{A}^{\mathrm{III}}\mathbf{e}_j\right)}{\lambda_i\lambda_j}\right] \tag{35}$$

3.2 Total potential energy

The specific elastic energy for a solid can be written as:

$$u_e(\boldsymbol{\varepsilon}) = \frac{1}{2}\boldsymbol{\varepsilon}^{\mathbf{T}}\mathbf{C}\boldsymbol{\varepsilon} = \frac{(K+2G)}{2}\left(\varepsilon_1^{\,2} + \varepsilon_2^{\,2} + \varepsilon_3^{\,2}\right) + K\left(\varepsilon_1\varepsilon_2 + \varepsilon_1\varepsilon_3 + \varepsilon_2\varepsilon_3\right) + \\ + \frac{G}{2}\left[\left(2\varepsilon_{12}\right)^2 + \left(2\varepsilon_{13}\right)^2 + \left(2\varepsilon_{23}\right)^2\right] \tag{36}$$

where $\boldsymbol{\varepsilon}$ is the stress measure shown in Eq.(34) and Eq.(35). Therefore, the potential elastic energy, given by Eq.(2) is rewritten as:

$$U_e = \int_{V_0} u_e(\boldsymbol{\varepsilon})\,dV_0 = \int_{V_0} \left\{ \frac{(K+2G)}{2}\left(\varepsilon_1^{\,2}+\varepsilon_2^{\,2}+\varepsilon_3^{\,2}\right) + K\left(\varepsilon_1\varepsilon_2+\varepsilon_1\varepsilon_3+\varepsilon_2\varepsilon_3\right) + \right.$$
$$\left. + \frac{G}{2}\left[(2\varepsilon_{12})^2 + (2\varepsilon_{13})^2 + (2\varepsilon_{23})^2 \right] \right\} dV_0 \tag{37}$$

By replacing Eq.(37) in Eq.(7), one has:

$$\Pi = \int_{V_0} \left\{ \frac{(K+2G)}{2}\left(\varepsilon_1^{\,2}+\varepsilon_2^{\,2}+\varepsilon_3^{\,2}\right) + K\left(\varepsilon_1\varepsilon_2+\varepsilon_1\varepsilon_3+\varepsilon_2\varepsilon_3\right) + \right.$$
$$\left. + \frac{G}{2}\left[(2\varepsilon_{12})^2 + (2\varepsilon_{13})^2 + (2\varepsilon_{23})^2 \right] \right\} dV_0 + \int_{V_0} \rho_0 \frac{\dot{x}_k \dot{x}_k}{2} dV_0 - F_i X_i + K_a \tag{38}$$

Eq.(38) represents the total potential energy in term of positions. The Newton-Raphason method and Newmark equations are used in order to solve the nonlinear problems as shown before.

3.3 FEM discretization

In this study, 20-node tetrahedral finite element are applied in the body discretization (See Figure 2).

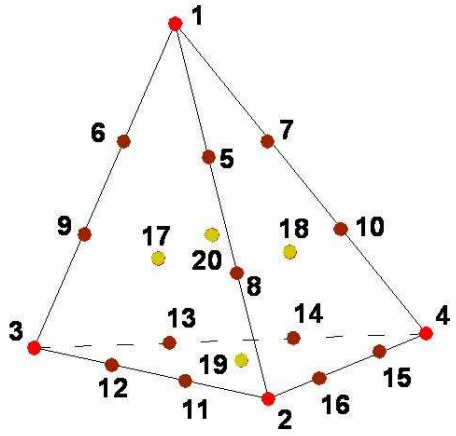

Figure 2: 20-node tetrahedral finite element

This discretization, which is isoparametric, performs cubic approximation for variables such as positions, velocities, accelerations and even stress field. These approximations are given by:

$$x_i(\xi_1,\xi_2,\xi_3) = \Phi_j X_i^j \tag{39}$$
$$\dot{x}_i(\xi_1,\xi_2,\xi_3) = \Phi_j \dot{X}_i^j \tag{40}$$
$$\ddot{x}_i(\xi_1,\xi_2,\xi_3) = \Phi_j \ddot{X}_i^j \tag{41}$$

where X_i^j, $\dot{X}_i^j$ and $\ddot{X}_i^j$ are nodal positions, velocities and accelerations respectively. Φ_j are the shape functions for tetrahedral finite element. Those shape functions can be found in, for example, Soriano (2003) and Zienkiewicz and Taylor (1991).

4 NUMERICAL EXAMPLES

4.1 Example 1: Clamped Bar submitted to an axial force

This example analyses the dynamic response of bar subjected to an axial load, according to Figure 3.

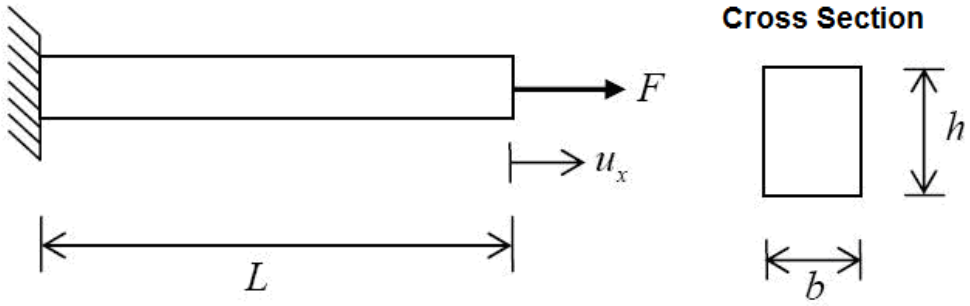

Figure 3: Beam under an axial load “F”.

A schematic graphic “Force vs time” is depicted in Figure 4 as well as the example data.

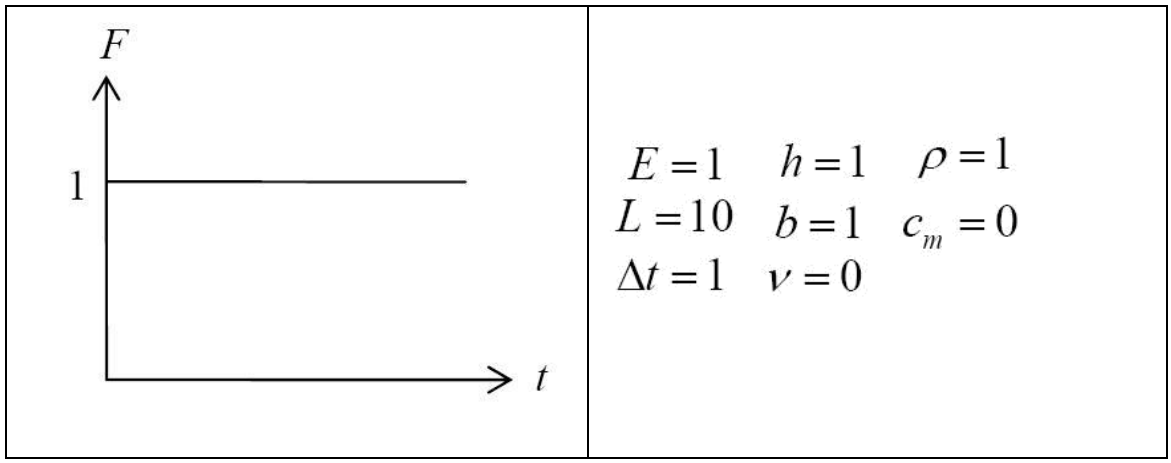

Figure 4: Graphic “Force x time” and example data.

Figure 5 shows the dynamic response for axial displacement u_x. Two different meshes have been used (463 nodes and 3329 nodes) in order to obtain the results and compared with the analytic response. In addition, for achieving good convergence, the Newmark parameters $\beta = 0.25$ and $\gamma = 0.5$ have been applied.

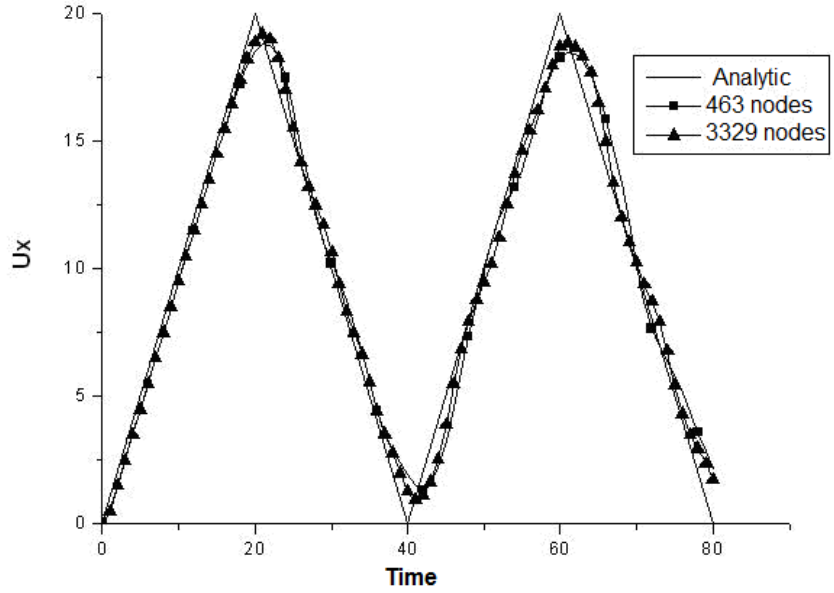

Figure 5: Dynamic response for horizontal displacement due to subit load.

It is impotant to observe (see Figure 5) the occurrence of some numerical damping, which has been expected. However, that numerical damping is reduced when the mesh is refined.

4.2 Example 2: Clamped beam submitted to a transversal force

In this example, a clamped beam is submitted to a transversal force, according to Figure 6. It is analyzed the dynamic response with and without damping.

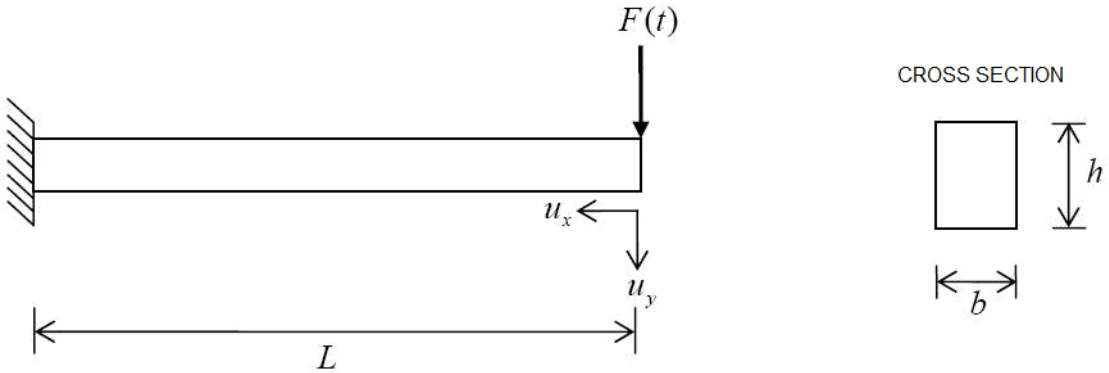

Figure 6: Clamped beam submitted to a transversal force in its free end.

Again, a schematic graphic “Force vs time” and the example data are depicted in Figure 7.

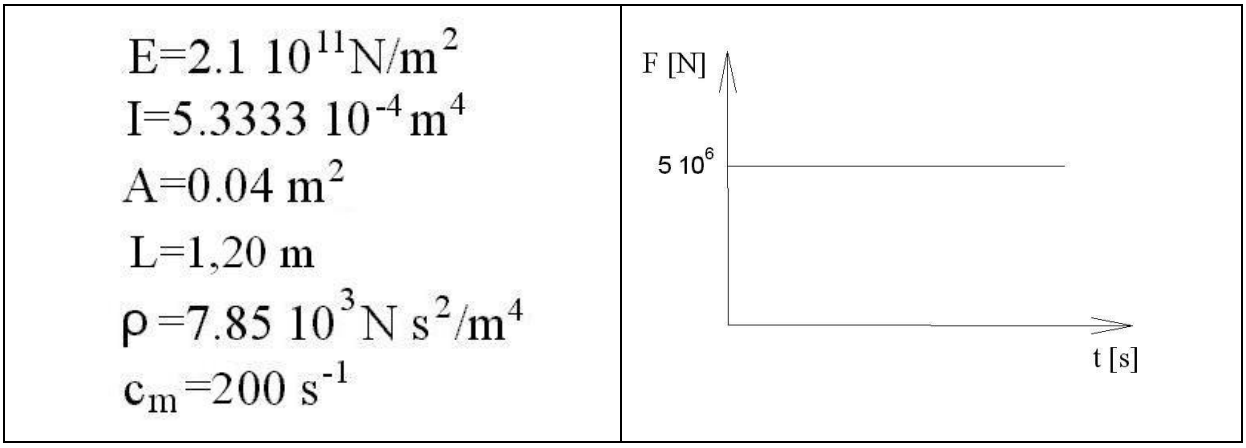

Figure 7: Problem data and "Force x time" grafic.

Figure 8 shows the dynamic response for the transversal displacement U_y. Two results are shown, including the static linear. The mesh is composed by 77 finite elements with $\Delta t = 0.0001$.

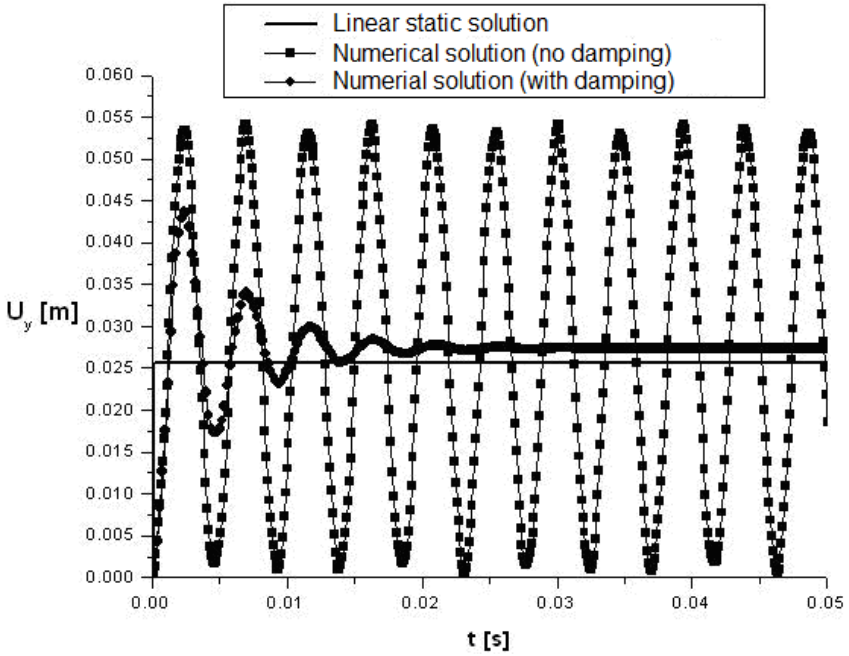

Figure 8: Dynamic response for the transversal displacement U_y versus time.

For damping response, the final displacements tend to the linear static one as already expected. But, since the static response do not consider the shear effects, it is natural to achieve more flexible results usnig FEM solid approach.

5 CONCLUSIONS

In this paper a consistent and simple formulation is proposed to solve geometrically non-linear dynamic problems involving solids. In order to show the didactic possibilities of the technique, a simple engineering language is used. Although the convergence is rather dependent on the Newmark parameters , the results obtained presents very good agreement

with those found in the specialized literature. For further developments, new time integration methods should be applied as well as different finite element shapes.

6 AKNOWLEDGEMENTS

The authors would like to thank CAPES and CNPq for the financial support.

REFERENCES

Armero F. and Garikipati K., An analysis of strong discontinuities in multiplicative finite strain plasticity and their relation with the numerical simulation of strain localization in solids. *International journal of solids and structures*, 33: 2863-2885, 1996

Haussy, B. and Ganghoffer, J. F., Instability analysis in pressurized transversely isotropic Saint-Venant-Kirchhoff and neo-Hookean cylindrical thick shells. *Arch. Appl. Mech.*, 74:600-617, 2005.

Hron, J and Mádlik, M., Fluid-structure interaction with applications in biomechanics. *Nonlinear analysis-real world applications*. 5:1431-1458, 2006.

Danielson, K. T. and Noor, A. K., Three-dimensional finite element analysis in cylindrical coordinates for nonlinear solid mechanics problems. *Finite elements in analysis and design*, 27: 225-249,1997.

Düster, A., Hartmann, S and Rank, E., p-FEM applied to finite isotropic hyperelastic bodies, *Comput. Methods Appl. Mech. Engrg*, 192: 5147-5166, 2003.

Bourdarias C., Gerbi S. and Ohayon J., A three dimensional finite element method for biological active soft tissue - Formulation in cylindrical polar coordinates. *Esaim-mathematical modelling and numerical analysis-modelisation mathematique et analyse numerique*, 37: 725-739, 2003.

Kožar, I. and Ibrahimbegović, A., Finite element formulation of the finite rotation solid element. *Finite elements in analysis and design*, 20: 101-126, 1995.

Maciel, D. N. and Coda, H. B.,Positional finite element method applied to geometric

nonlinear tridimensional problems, *Cadernos de Engenharia de Estruturas*, 11-111-130, 2009.

Moita, G. F. and Crisfield, M. A., A finite element formulation for 3-D continua using the co-rotational technique. *Int. J. of Num. Meth. In Eng*., 39: 3775-3792., 1996

Ogden, R. W., *Non-linear elastic deformation*. Chichester, Ellis Horwood, 1984.

Rank, E., Bröker, H., Düster, A., Krause, R. and Rücker, M., The p-version of the finite element method for structural problems. *Error-Controlled Adaptive Finite Elements in Solid Mechanics, John Wiley & Sons*, 263–307, 2002.

Reese, S., Küssner, M and Reddy, B. D., A new stabilization technique for finite elements in non-linear elasticity. *Int. J. Numer.Methods Eng*., 44: 1617–1652, 1999.

Simo, J. and Armero, F., Geometrically non-linear enhanced strain mixed methods and the method of incompatible modes. *Int. J. Numer. Methods Eng*., 33: 413–1449, 1992

Simo J.C., Armero F. and Taylor R.L., Improved versions of assumed enhanced strain tri-linear elements for 3d-finite deformation problems. *Computer methods in applied mechanics and engineering*, 110: 359-386, 1993

SORIANO, H. L., *Método de Elementos Finitos em Análise de Estruturas*. São Paulo: Edusp - Editora da Universiadade de São Paulo, 2003.

Zienkiewicz, O.C., and Taylor, R.L., *The finite element method*, volume II. McGraw Hill, 1991.